Optical-Model Analysis of Pion-Nucleus Scattering

E. H. AUERBACH*
Brookhaven National Laboratory, Upton, New York

AND

D. M. FLEMING† AND M. M. STERNHEIM†
Department of Physics and Astronomy, University of Massachusetts, Amherst, Massachusetts

(Received 16 June 1967)

Determination of nuclear-density parameters and of the rms pion charge radius r_π from the elastic scattering of pions by nuclei has been studied using the optical model proposed by Kisslinger. Good fits to the available data in the kinetic-energy region 24 MeV$\leq T_\pi \leq$153 MeV have been found by searching the parameter space. For $T_\pi \approx 80$ MeV, i.e., T_π large compared to nuclear binding energies but well below the N^* resonance, the best-fit parameters are close to those predicted from pion-nucleon phase shifts. The nuclear radii obtained are consistent with electron-scattering radii; the calculated differential cross sections are sensitive to a second nuclear-density parameter for large angles. "Distortion" of the Coulomb amplitude in 24-MeV $\pi^\pm$-α scattering reduces r_π from 1.8±0.8 F to $r_\pi \leq 2.0$ F (two standard deviations), in agreement with West's recent calculation.

I. INTRODUCTION

IN this paper we present the results of a systematic optical-model analysis of low-energy elastic pion-nucleus scattering.[1] Our primary goal was the development of a method of extracting the root-mean-square (rms) pion charge radius r_π from $\pi^\pm$-α elastic scattering, as proposed recently.[2] Another objective was to explore the use of pions as nuclear-density probes. All available experimental data of sufficient precision in the laboratory kinetic-energy region 24 MeV$\leq T_\pi \leq$153 MeV were studied. These include scattering by helium and carbon at several energies, and by lithium, aluminum, copper, and lead at one or two energies.

Other methods have been proposed and applied to studying the electromagnetic structure of the pion. Elastic π-e scattering[3] has given $r_\pi \leq 3.0$ F. Electroproduction of the π^+ in the reaction $e^-+p \rightarrow e^-+n+\pi^+$, when analyzed with a one-photon exchange model, gives[4]

$$r_\pi = 0.66_{-0.31}{}^{+0.26} \text{ F}, \tag{1}$$

in good agreement with the $r_\pi = 0.6$ F obtained by assuming that the pion couples to the photon through the exchange of ρ^0. However, both of these methods have sufficient experimental and theoretical difficulties to justify seeking alternative approaches to the pion structure problem.

For a $T=0$ nucleus such as the α particle, the amplitude $f_N(\theta)$ for scattering by the purely nuclear forces is the same for π^+ and π^-. Using the Born approximation $f_C{}^B$ for the Coulomb amplitude, the differential cross section for elastic $\pi^\pm$ scattering is

$$\frac{d\sigma^\pm}{d\Omega}(\theta) = |f_N(\theta) \pm f_C{}^B(\theta)|^2. \tag{2}$$

Thus the difference of cross sections $D = d\sigma^-/d\Omega - d\sigma^+/d\Omega = -4\,\mathrm{Re}(f_N{}^* f_C{}^B)$ is linear in the Coulomb amplitude. An estimate for f_N was obtained using the single scattering (or impulse) approximation, together with approximate multiple scattering calculations of dubious validity at large angles. From this estimate, it was concluded[2] that at 100 MeV D is sensitive to deviations from the point Coulomb amplitude near the minimum in f_N occurring at about 75°. It was also suggested that an optical-model analysis would be needed to extract the small deviations caused by the charge structures of the π and α.

At first inspection this optical-model analysis might not seem necessary. Nordberg and Kinsey,[5] for example, recently published their measurements and analysis of 24-MeV $\pi^\pm$-α scattering. They used a partial-wave expansion for f_N with complex phase shifts for $l=0$ and 1, and a real phase shift for $l=2$. For the Coulomb amplitude, they multiplied the point Coulomb Born $f_{C0}{}^B$ approximation by $(1-q^2r^2/6)$. Fitting the six free parameters to their data gave

$$r_\pi = (r^2 - r_\alpha{}^2)^{1/2} = 1.8 \pm 0.8 \text{ F}. \tag{3}$$

However, this analysis does not include all the contributions to the amplitude which are linear in the Coulomb potential, as was emphasized by Schiff.[6] The incident wave on which the Coulomb potential operates is distorted by the nuclear forces. (Alternatively, one

* Supported by the U. S. Atomic Energy Commission.
† Supported in part by the National Science Foundation.

[1] A preliminary account of some of this work was given by M. M. Sternheim and E. H. Auerbach, in Proceedings of the Williamsburg Conference on Intermediate Energy Physics, Williamsburg, Virginia, 1966, p. 439 (unpublished). The results given were inaccurate because of an error in the computer program.

[2] M. M. Sternheim and R. Hofstadter, Nuovo Cimento **38**, 1854 (1965).

[3] D. G. Cassel, Ph.D. thesis, Princeton University, 1965 (unpublished).

[4] C. W. Akerlof, W. W. Ash, R. Berkleman, and C. A. Lichtenstein, Phys. Rev. Letters **16**, 528 (1966).

[5] M. E. Nordberg and K. F. Kinsey, Phys. Letters **20**, 692 (1966).

[6] L. I. Schiff, Progr. Theoret. Phys. (Kyoto) Suppl., Extra Number, 400 (1965). See also, M. Ericson, Nuovo Cimento **47**, 49 (1967).

can say that f_N is not the same for π^+ and π^-, since the Coulomb potential distorts the incident wave on which the nuclear forces operate.) Thus there is an additional distortion term $\pm f_D$ which has to be included in Eq. (1). It must be estimated, e.g., by use of an optical potential, before a phase-shift analysis can be employed.

The $l=0$ part of f_D is particularly important; for with $f_{C0}{}^B \sim q^{-2}$, we have

$$\Delta f_C \equiv f_C - f_{C0} \sim q^{-2}(1-q^2r^2/6) - q^2 \sim -r^2/6. \quad (4)$$

Thus the largest effect[7] on $\pi^{\pm}$-α scattering of a deviation from the point Coulomb potential is a sign-changing s-wave amplitude proportional to r^2. The s-wave part of f_D can be comparable to the contribution of the pion radius, and therefore may not safely be neglected; distortions in other partial-waves may also alter the analysis significantly. Very recently, West has applied a simplified optical model[8] to the 24-MeV data, and has found that the inclusion of distortion changes the result from $r_\pi = 1.8 \pm 0.8$ F to $r_\pi \leq 1.5$ F.

Another incentive to undertaking these calculations was the general lack of detailed pion-nucleus elastic scattering calculations in the published literature. It was not initially clear whether good over-all fits to experimental data could be obtained with either theoretical or phenomenological models and parameters. Despite the considerable amount of theoretical work by Watson[9] and others, most existing calculations did not yield full agreement with experiment. Optical potentials proportional to the nuclear density $\rho(r)$ give good results for small angles, using well depths close to those predicted from π-nucleon phase shifts.[10] However, these depths cannot be adjusted to fit experimental data for large angles. Similarly, approximate multiple scattering calculations[11] using π-nucleon data and electron-scattering nuclear-density functions fit only to the region of the first minimum.

The velocity-dependent optical potential derived by Kisslinger[12] would appear on theoretical grounds to have considerable promise. It has been applied so far only in a modified form by Rainwater and his coworkers,[13,14] who analyzed their several experiments around 80 MeV, and were able to fit their data quite well. The modification of the Kisslinger model makes it difficult to compare their phenomenological well parameters with the corresponding two-body data. West[8] also used this modified model. To date, no calculations have been published based on the original Kisslinger model.

Thus independently of the pion form factor problem, it appeared quite interesting to study the Kisslinger model in its original form. Much better pion-nucleus experiments are becoming feasible, and pions are likely to be quite useful as nuclear probes.[15] Therefore, we set out to answer these questions: (1) Does the Kisslinger model work, i.e., can a set of parameters always be found which leads to the observed elastic scattering? (2) Do the "best-fit" optical-model parameters obtained by searching the parameter space agree with the "theoretical" parameters calculated from π-nucleon phase shifts or at least vary reasonably with the nuclear mass A and with T_π? (3) Are the "best-fit" nuclear-density parameters consistent with electron scattering experiments? (4) Can unique values be obtained for f_D, the distortion amplitude in π-α scattering?

In the next section we summarize the derivation and limitations of the Kisslinger model. In Sec. III we compare the best-fit and theoretical parameters, as well as the measured and computed cross sections. Applications to nuclear density and radius determinations and to the pion form factor are discussed in Secs. IV and V, respectively.

II. OPTICAL-MODEL DERIVATION

We summarize briefly Watson's derivation[9] of the optical model. Consider a pion incident upon a nucleus of A nucleons. The Hamiltonian is

$$H = (H_N + h) + \sum_{i=1}^{A} V_i \equiv H_0 + V,$$

where H_N is the nuclear Hamiltonian, h is the pion kinetic energy operator, and V_i is the π-nucleon potential. The scattering amplitude T is a solution of

$$T = V + Va^{-1}T, \quad (5)$$

where $a = E - H_0 + i\epsilon$. An exact formal solution of Eq. (5) is

$$T = \sum_i t_i' + \sum_{ij}{}' t_i' a^{-1} t_j' + \sum_{ijk}{}' t_i' a^{-1} t_j' a^{-1} t_k' + \cdots, \quad (6)$$

where t_i' is the amplitude for pion-bound nucleon scattering. $\sum'$ means that two successive scatterings by a single nucleon are to be excluded.

The "coherent part" θ_C of an operator θ is defined by

$$\langle \gamma' | \theta_C | \gamma \rangle = \langle \gamma' | \theta | \gamma \rangle \quad \text{if} \quad W_\gamma = W_{\gamma'}, \quad (7)$$
$$= 0 \quad \text{if} \quad W_\gamma \neq W_{\gamma'},$$

[7] This was first pointed out to us by M. Block who attributes the observation to Cabibbo. It has also been discussed by M. Ericson (Ref. 6).

[8] G. B. West, Phys. Rev. (to be published). His analytic nonrelativistic calculation uses a uniform sphere nuclear density and the modified Kisslinger model which we discuss at the end of Sec. II.

[9] K. M. Watson, Rev. Mod. Phys. **30**, 565 (1958); also earlier papers given here.

[10] L. D. Roper and R. M. Wright, University of California Radiation Laboratory Report No. UCRL 7846, 1964 (unpublished); L. D. Roper, R. M. Wright, and B. T. Feld, Phys. Rev. **138**, B190 (1965), solutions 14 and 24.

[11] M. M. Sternheim, Phys. Rev. **135**, B912 (1964).

[12] L. S. Kisslinger, Phys. Rev. **98**, 761 (1955).

[13] W. F. Baker, J. Rainwater, and R. E. Williams, Phys. Rev. **112**, 1763 (1958); W. F. Baker, H. Byfield, and J. Rainwater, *ibid.* **112**, 1773 (1958).

[14] R. M. Edelstein, W. F. Baker, and J. Rainwater, Phys. Rev. **122**, 252 (1961).

[15] M. Ericson and T. Ericson, Ann. Phys. (N. Y.) **36**, 323 (1966).

where W_γ is the nuclear energy. Thus the elastic scattering amplitude is

$$T_C=t_i'C+\sum'(t_i'a^{-1}t_j')C+\cdots. \tag{8}$$

The optical potential $\mathcal{U}$ in analogy with Eq. (5) is defined by

$$T_C=\mathcal{U}+\mathcal{U}a^{-1}T_C. \tag{9}$$

Thus, formally at least, calculating the pion-nucleus elastic scattering has been reduced to solving a one-particle problem with the Hamiltonian $h+\mathcal{U}$.

Useful expressions for $\mathcal{U}$ can be obtained if sufficient approximations are made. Neglecting excited nuclear states, we have

$$(t_i'a^{-1}t_j'\cdots)_C=t_i'Ca^{-1}t_j'C\cdots.$$

If A is large or if the two-body forces are weak, we can set $\sum'=\sum$. Then Eq. (8) implies

$$T_C=\sum t_i'C=\sum t_i'Ca^{-1}T_C \tag{10}$$

or

$$\mathcal{U}=\sum t_i'C. \tag{11}$$

The impulse approximation, or the replacement of the bound amplitudes t_i' by the free π-nucleon amplitudes t_i, is reasonable for energies large compared to nuclear binding energies. If the nucleon recoil is also neglected, Eq. (11) becomes

$$\langle\mathbf{p}'|\mathcal{U}|\mathbf{p}\rangle=\sum_i\langle\mathbf{p}'|t_i|\mathbf{p}\rangle\rho(\mathbf{p}'-\mathbf{p}), \tag{12}$$

where $\mathbf{p}'$ and $\mathbf{p}$ are the pion momenta. Here

$$\rho(\mathbf{q})\equiv\int e^{i\mathbf{q}\cdot\mathbf{r}}\rho(\mathbf{r})d^3r \tag{13}$$

is the nuclear form factor or Fourier transform of the nuclear density function, which is normalized to unity:

$$\int\rho(\mathbf{r})d^3r=1. \tag{14}$$

The approximation of neglecting recoil is apparently not very good[16] for off-shell matrix elements of $\mathcal{U}$, which contribute significantly to large-angle scattering.[11]

The simplest optical model is obtained from Eq. (12) with a forward scattering approximation for t:

$$\langle\mathbf{p}'|t|\mathbf{p}\rangle\rho(\mathbf{p}'-\mathbf{p})\approx\langle\mathbf{p}|t|\mathbf{p}\rangle\rho(\mathbf{p}'-\mathbf{p})\approx\langle\mathbf{p}_0|t|\mathbf{p}_0\rangle\rho(\mathbf{p}'-\mathbf{p}).$$

Here one assumes first that $\rho(q)$ drops off rapidly with increasing q, and then that the wave function in momentum space is strongly peaked about the incident momentum $\mathbf{p}_0$. In coordinate space, $\mathcal{U}$ is now a local potential

$$\mathcal{U}(\mathbf{r})=(2\pi)^3A\langle\mathbf{p}_0|t|\mathbf{p}_0\rangle\rho(\mathbf{r}), \tag{15}$$

where $\langle\mathbf{p}_0|t|\mathbf{p}_0\rangle$ is suitably averaged over π-p and π-n amplitudes. Calculations based on this simple model invariably fit only small-angle data, as noted in the Introduction.[13,17,18]

This model fails to take into account the largely p-wave character of low-energy π-nucleon scattering. Noting that usually $t_l\sim p^{2l}$ holds, Kisslinger[12] substituted into Eq. (12)

$$\langle\mathbf{p}'|t|\mathbf{p}\rangle=a_0+a_1p^2\cos\theta=a_0+a_1\mathbf{p}'\cdot\mathbf{p}, \tag{16}$$

obtaining

$$\langle\mathbf{r}|\mathcal{U}\psi\rangle=(2\pi)^3A[a_0\rho\psi-a_1\nabla\cdot(\rho\nabla\psi)], \tag{17}$$

or, in terms of momentum operators,

$$\mathcal{U}(\mathbf{r})=(2\pi)^3A[a_0\rho+a_1\mathbf{p}\cdot\rho\mathbf{p}]. \tag{18}$$

We shall see shortly that Eq. (16) is fairly consistent with experimental (i.e., on the energy shell) π-nucleon scattering at kinetic energies well below the N^* resonance near 200 MeV. However, its validity for $|\mathbf{p}|\neq|\mathbf{p}'|$ is unknown, and it clearly violates unitarity for large momenta. Furthermore, at best only a small region near $T_\pi=(20\times200)^{1/2}=65$ MeV is compatible with Eq. (16) and also with the impulse approximation.

The loss of pions from the elastic channel is proportional to

$$-\int\psi^*(\mathcal{U}-\mathcal{U}^+)\psi d^3r=2(2\pi)^3A\times\int\mathrm{Im}[a_0|\psi|^2+a_1|\nabla\psi|^2]\rho d^3r. \tag{19}$$

Since $\rho\geq0$, both terms in Eq. (18) always correspond to sinks (sources) of pions if Im a_0 and Im a_1 are negative (positive). For spin zero, Eq. (18) is the simplest velocity-dependent potential having this property which is consistent with the usual symmetries.

Following Baker *et al.*[13], we introduce $\mathcal{U}$ into a Klein-Gordon equation as a fourth component of a four-vector and drop the $\mathcal{U}^2$ term. Thus if V_C is the Coulomb potential

$$(-\nabla^2+\mu^2)\psi=(E_\pi-V_C-\mathcal{U})^2\psi\approx[(E_\pi-V_C)^2-U]\psi. \tag{20}$$

This is the equation we actually solve. With Eq. (18),

$$U\psi=2E_\pi\mathcal{U}\psi=-Ab_0p_0^2\rho\psi+Ab_1\nabla\cdot(\rho\nabla\psi), \tag{21}$$

where

$$b_0=-2(2\pi)^3E_\pi a_0/p_0^2,\qquad b_1=-2(2\pi)^3E_\pi a_1. \tag{22}$$

The b's are proportional to π-nucleon amplitudes and

[16] E. Leader, Nucl. Phys. **26**, 177 (1961).

[17] T. A. Fujii, Phys. Rev. **113**, 695 (1959).

[18] Yu. A. Budagov, P. F. Ermolov, E. A. Kushnirenko, and V. I. Moskalev, Zh. Eksperim. i Teor. Fiz. **42**, 1191 (1961) [English transl.: Soviet Phys.—JETP **15**, 824 (1962)].

are independent of nuclear parameters; they differ from the C's of Baker *et al.*[13] by a factor $-A\rho(0)$.

We must relate the optical potential in the lab system to phase shifts in the π-nucleon center-of-mass system. Let k be the pion momentum in this c.m. system. The usual connection between t and $f(\theta)$ gives

$$\langle \mathbf{p}|t|\mathbf{p}\rangle_{\text{lab}} = -f(0)_{\text{lab}}/(4\pi^2 E_\pi). \tag{23}$$

With the optical theorem and the invariance of total cross sections,

$$f(0)_{\text{lab}}/p = f(0)_{\text{c.m.}}/k. \tag{24}$$

Thus we obtain readily for $l=0$, 1

$$\begin{aligned} b_l &= \frac{4\pi}{pk^2}[kf(0)_{\text{c.m.}}]_l \\ &= \frac{4\pi}{p^3}\frac{\mu^2+M^2+2E_\pi M}{M^2}[kf(0)_{\text{c.m.}}]_l, \end{aligned} \tag{25}$$

where μ and M are the pion and nucleon masses, respectively.

The amplitudes in Eq. (25) must be suitably averaged, over spin and isospin variables. Let $\alpha_i = \exp(i\delta_i)\sin\delta_i$, where the δ_i are the π-nucleon phase shifts and $i=(2T,2J)$. For a π^- and a nucleus (A,Z), we find

$$\begin{aligned} [kf(0)_{\text{c.m.}}]_0 &= [Z(\alpha_3+2\alpha_1)/3+(A-Z)\alpha_3]A^{-1}, \\ [kf(0)_{\text{c.m.}}]_1 &= [Z(2\alpha_{33}+\alpha_{31}+4\alpha_{13}+2\alpha_{11})/3 \\ &\quad +(A-Z)(2\alpha_{33}+\alpha_{31})]A^{-1}. \end{aligned} \tag{26}$$

For π^+ scattering, the factors Z and $(A-Z)$ are interchanged.

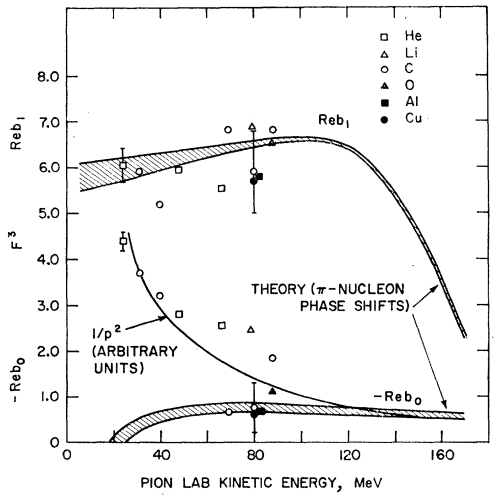

FIG. 1. Theoretical and phenomenological best-fit values for the real parts of the optical-model well-depth parameters b_0 and b_1. The bands of theoretical values indicate the extremes of those calculated for $A=2Z$ nuclei from the three sets of pion-nucleon phase shifts listed in Ref. 10. The error bars shown were obtained by an error-matrix analysis, as described in the text; other best-fit values probably have similar errors. For π^--lithium, the best-fit Re b_1 has been reduced by Re $(b_1)_{A=4,\ Z=3} - \text{Re}(b_1)_{A=2Z} = 0.7$, and $|\text{Re}\ b_0|$ has been similarly reduced by 0.4.

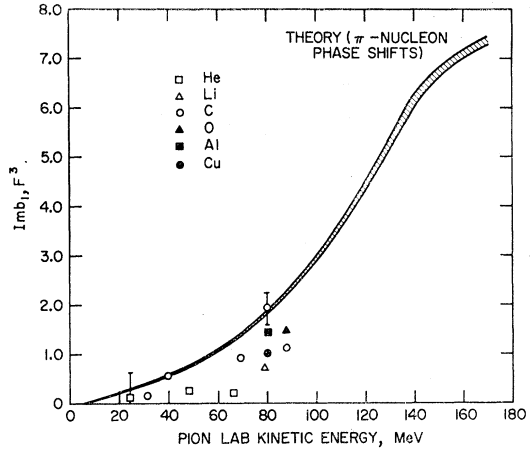

FIG. 2. Theoretical and phenomenological best-fit values for the imaginary part of the optical-model well-depth parameter b_1. The theoretical values and error bars are obtained as for Fig. 1. The best-fit value for lithium has been reduced by $\text{Im}(b_1)_{A=4,\ Z=3} - \text{Im}(b_1)_{A=2Z} = 0.3$.

We used three different sets of phenomenological π-nucleon phase shifts obtained by Roper *et al.*[10] to evaluate b_0 and b_1. They give similar but not identical results, as is seen in Figs. 1–3 plotted for the case $A=2Z$. Since b_1 is dominated by $\alpha_{33}/p^3 \approx (\delta_{33}+i\delta_{33}^2)/p^3$ and δ_{33} has the expected p^3 behavior, we find Re b_1 is almost constant at about 6.3 for $T_\pi \leq 130$ MeV.[19] Hence Im b_1 is rapidly increasing; it is 0.2 at 20 MeV, 1.8 at 80 MeV, and 6.8 at 150 MeV. The empirical leading terms[10] linear in p in $2\delta_3$ and in δ_1 nearly cancel, so that Re $b_0 \sim (2\delta_3+\delta_1)/p^3$ is surprisingly constant at -0.7 except at very low energies; one expected a $1/p^2$ behavior. Im $b_0 \sim (2\delta_3^2+\delta_1^2)/p^2$ has the expected $1/p$ dropoff from a value of 0.6 at 25 MeV.

From this discussion, it is clear that the largest theoretical uncertainty is associated with Re b_0, since moderate deviations from the free pion-nucleon amplitudes may spoil the accidental cancellations and lead thereby to much larger values and to a $1/p^2$ variation.

A few remarks are in order before concluding this section. We have not included corrections for the "effective kinetic energy" of the pion inside the nucleus,[20] for the Lorentz-Lorenz effect,[15,21] and for pion capture.[15,20] Our actual calculations are made in the π-nucleus c.m. frame; we neglect the small effects on the theoretical parameters of the transformation from the lab frame.

The modified Kisslinger model mentioned in the Introduction is obtained from the above by the replacement

$$(1+b_1\rho A)\nabla^2\psi \rightarrow (1-Ab_1\rho)^{-1}\nabla^2\psi.$$

[19] All radii are given in fermis; the b's have units of F^3.

[20] R. M. Frank, J. L. Gammel, and K. M. Watson, Phys. Rev. **101**, 891 (1956).

[21] N. M. Kroll, quoted in Ref. 14.

TABLE I. Best-fit parameters for 80-MeV π^--C scattering.

Density	Reb_0 (F^3)	Imb_0 (F^3)	Reb_1 (F^3)	Imb_0 (F^3)	$\bar{r}$ (F)
Saxon-Woods, $R=2.45\text{F}\pm0.11\text{F}$, $c=0.25\text{F}$	-0.75 ± 0.54	0.28 ± 0.87	5.91 ± 0.93	1.94 ± 0.30	2.11 ± 0.10
Saxon-Woods, $R=1.97\text{F}$, $c=0.45\text{F}$	-1.24	0.22	6.41	1.44	2.26
Modified Gaussian, $a=1.47\text{F}$	-1.14	0.22	6.16	1.32	2.14
Theory (2-body phase shift)	-0.75 ± 0.10	0.34 ± 0.02	$6.5\ \pm0.1$	$1.8\ \pm0.1$	

Since Im $b_1\neq0$, this replacement is not needed to avoid singular points. It introduces a further difficulty in comparing phenomenological and theoretical parameters. We have used this model only to help verify our computer programs: we obtain good agreement with the older calculations.[13]

III. CALCULATIONS

The solutions of the optical-model wave equation, Eq. (20), were obtained using a suitable modification of the ABACUS code originally developed by one of us for nonrelativistic velocity-independent optical potentials.[22] For each partial wave required the program solves for the wave functions using difference equations with as many as 500 mesh points. These are joined to solutions of the Klein-Gordon point Coulomb equation outside the nuclear force region.

ABACUS can "scan" parameter sets, i.e., repeat the calculations for systematically varied parameters. It can also perform gradient searches to find "best-fit" parameter values which minimize χ^2 for a given set of experimental data. An average of about 1 sec was required to solve a set of partial-wave equations on a large digital computer. Several hours of computer time were needed to do the various scans and searches discussed below.

Two different nuclear-density functions were used:

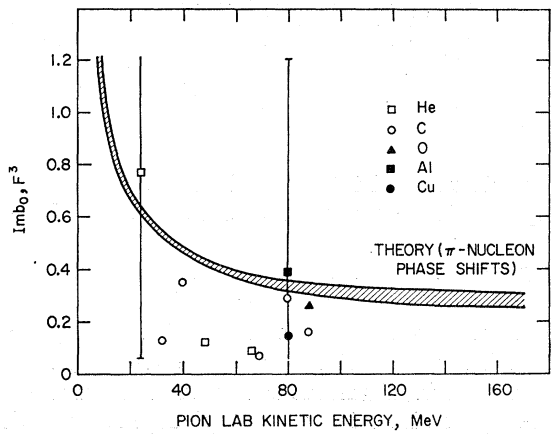

FIG. 3. Theoretical and phenomenological best-fit values for the imaginary part of the optical-model well-depth parameter b_0. The theoretical values and error bars are obtained as for Fig. 1. The best-fit Im b_0 for π^--lithium is omitted; it is -0.95.

[22] E. H. Auerbach, Brookhaven National Laboratory Report No. BNL 6562, 1962 (unpublished).

(1) the modified Gaussian

$$\rho_G(r)=\rho_0[1+(Z-2)r^2/3a^2]\exp(-r^2/a^2),\qquad \rho_0=2/\pi^{3/2}a^3Z. \tag{27}$$

This density is obtained from shell-model wave functions for the $1p$ shell nuclei, and is consistent with electron scattering experiments on these nuclei.[23] (2) the familiar Saxon-Woods density[24]

$$\rho_s(r)=\rho_0[1+\exp(r-R)/c]^{-1},\qquad \rho_0\approx(3/4\pi R^3)(1+\pi^2c^2/R^2)^{-1}. \tag{28}$$

Both densities were set exactly equal to zero once they had reached very small values. For the Coulomb potential, we used as the charge distribution a modified Gaussian with ρ_G, and either a uniform sphere or modified Gaussian with ρ_s. The corresponding charge radius parameters are referred to below as a_c and R_c, respectively.

A. Phenomenological Best-Fit Parameters

We began by studying elastic scattering of pions by helium and carbon for $24\leq T_\pi\leq92$ MeV. Since a principal objective was to determine the uniqueness of the optical potential, we "mapped" the parameter space, i.e., obtained χ^2 for many values of the complex constants b_0 and b_1. The theoretical parameters were used only to determine suitable orders of magnitude for initial investigation. The search program was used to locate χ^2 minima more precisely once their approximate positions were found in these scans. Nuclear-density parameters were also varied in some cases; this will be discussed in Sec. IV.

We selected two representative experiments and performed an error analysis on the corresponding best fits. We assumed that χ^2 depends quadratically on the parameters near its minimum, and computed the error matrix in the usual way. The best-fit b's are strongly correlated to each other, but not to the nuclear-density parameters; this would not have been true had we used the C's of Baker *et al.*[13] The standard deviations thus obtained provide a crude estimate of the errors associated with the best-fit parameters for other experiments.

For no helium or carbon experiments was more than one region of good fit found in the scans. Although searches sometimes found equally good fits with two or more parameter sets these sets always agreed within the estimated errors. This is illustrated in Table I.

[23] D. G. Ravenhall, Rev. Mod. Phys. **30**, 430 (1958).

[24] P. E. Hodgson, *The Optical Model of Elastic Scattering* (Clarendon Press, Oxford, England, 1963).

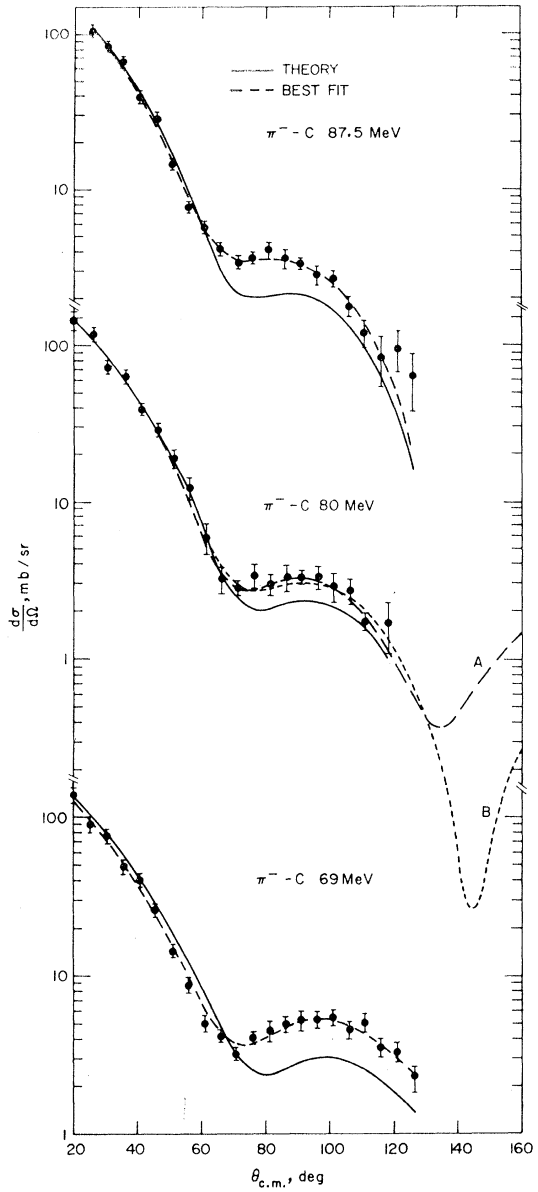

FIG. 4. π^--carbon elastic scattering at 69.5, 80, and 87.5 MeV. The 80-MeV experimental data are those of Baker *et al.* (Ref. 13) and the others were obtained by Edelstein *et al.* (Ref. 14). The solid curves give our cross sections calculated with theoretical parameters which in some cases differ by amounts which are not significant from those of Fig. 1–3; these are $b_0=-0.66+0.41\ i$ $b_1=6.30+1.30\ i$ for 69.5 MeV, $b_0=-0.62+0.39\ i$, $b_1=6.30+1.70\ i$ for 80 MeV, and $b_0=-0.63+0.36\ i$, $b_1=6.30+1.85\ i$ for 87.5 MeV. The dashed curves give the best fits obtained by varying both well depths and nuclear-density parameters. The best-fit b's are $b_0=-0.66+0.73i$, $b_1=6.81+0.93i$ for 69.5 MeV, (A) $b_0=-0.75+0.28i$, $b_1=5.91+1.94i$ and (B) $b_0=-1.24+0.23i$, $b_1=6.41+1.44i$ for 80 MeV, and $b_0=-1.83+0.16i$, $b_1=6.83+1.11i$ for 87.5 MeV. All the theoretical curves are computed using modified Gaussian nuclear densities with the same radii as in the best modified Gaussian fits, i.e., 1.47, 1.47, and 1.49 at 69.5, 80, and 87.5 MeV, respectively. The best-fit modified Gaussian 80-MeV cross section is omitted, since it is very much like the plotted Saxon-Woods curve (B) which has $R=1.97$, $c=0.45$. Both of these differ considerably at large angles from the curve (A) obtained with $R=2.45$, $c=0.25$. The nuclear charge density used in all cases is a modified Gaussian with $a_c=1.6$.

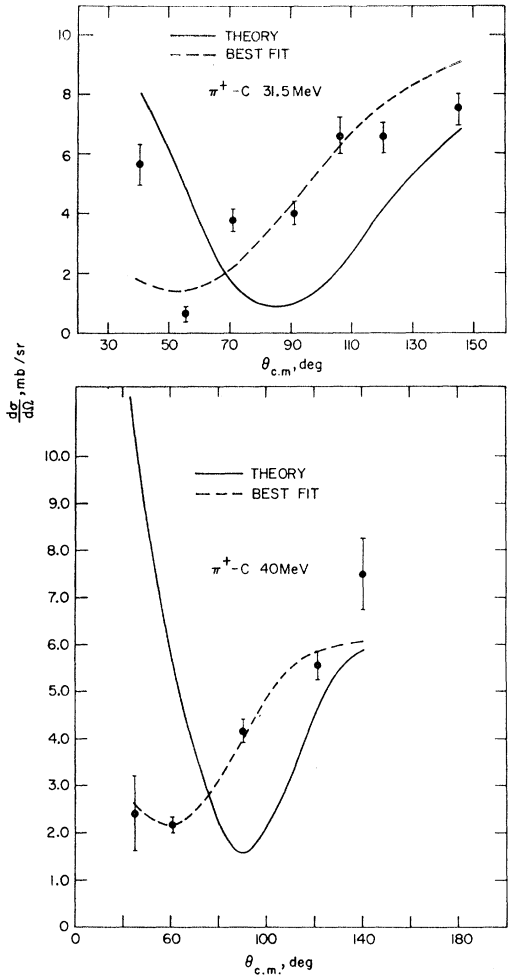

FIG. 5. π^+-carbon elastic scattering at 31.5 and 40 MeV. The experimental data are those of Kane (Ref. 25) and Perry (Ref. 26), respectively. Theoretical parameters used are $b_0=-0.50+0.53i$, $b_1=6.30+0.40i$ for 31.5 MeV, and $b_0=-0.80+0.50i$, $b_1=6.30+0.55i$ for 40 MeV. Best-fit parameters are $b_0=-3.71+0.13i$, $b_1=5.90+0.16i$ for 31.5 MeV, and $b_0=-3.20+0.35i$, $b_1=5.20+0.55i$ for 40 MeV. The nuclear density and charge distribution used are modified Gaussians with $a=a_c=1.6$; these radii were not varied.

Experiments on Li, O, Al, and Cu near 80 MeV were analyzed using searches started from the carbon best-fit parameters.

Figures 1–3 summarize the results of these parameter searches. The largest parameter, Re b_1, is very close to the predicted value in all cases. Im b_0 is small, as expected, but the associated errors are very large. Re b_0 is very large in magnitude compared to the theoretical value, approaching it with a $1/p^2$ dependence as T_π increases; we noted this possibility in Sec. II. Im b_1 is somewhat smaller than predicted for most nuclei; for He, it is very small. The reason for this is not apparent. Note, however, that the larger nuclear density of He makes the replacement of free amplitudes for bound amplitudes less valid.

In short, the phenomenological best-fit parameters below 100 MeV are for the most part consistent with the pion-nucleon data, vary smoothly with T_π, and are nearly independent of A. They are quite close to the predicted values for $T_\pi \sim 80$ MeV, as expected from our arguments in Sec. II.

B. Experimental Comparison

We now examine more closely the agreement between our calculations and the available data, considering first $T_\pi < 100$ MeV. Slightly inelastic scattering due to excitation of low-lying nuclear levels complicates the elastic-scattering experiments. Some inelastic cross sections increase rapidly with momentum transfer and become much greater than large-angle elastic-scattering cross sections. In some experiments the unresolved inelastic contamination is so large that the reported cross sections are useful only as upper bounds on the large-angle elastic scattering, despite the small statistical errors quoted.

Carbon: Since the first excited state is 4.4 MeV above the ground state, the separation of elastic events is feasible. Useful π^+ data are available at 31.5 MeV[25] and 40 MeV,[26] and π^- data at 69.5 MeV,[14] 80 MeV,[13] and 87.5 MeV.[14] In Fig. 4, we see that for the three higher energies ρ_G and the theoretical parameters give results very close to the experimental data; the slightly different best-fit parameters give $\chi^2/N \lesssim 1$, where N is the number of data points.

At the lower energies the theoretical parameters give curves of the right qualitative behavior, but they are too high in front and too low in back. In the Born approximation, $f(\theta) \sim b_0 + b_1 \cos\theta$. Since Re b_0 is negative and Re b_1, Im b_1, and Im b_0 are positive, increasing $|\mathrm{Re}\, b_0|$ will improve the fit. The search yields relatively large values of $|\mathrm{Re}\, b_0|$ and good fits to the data. Both experiments have poor statistics and our search program was relatively ineffective. See Fig. 5.

Oxygen: Pure elastic π^--oxygen scattering has been measured at 87.5 MeV.[14] The theroetical parameters and ρ_G yield an excellent fit; the best-fit parameters improve the fit slightly. See Fig. 6.

Aluminum, copper: The 80-MeV π^- measurements on these nuclei[13] contain some inelastic events. Figure 6 gives our results with ρ_s and theoretical parameters, which are consistent with the data if they are treated as upper bounds. Excellent fits can be obtained if one assumes the measured cross sections are purely elastic.

Lithium: $\pi^\pm$-lithium scattering was first measured[27] with relatively poor energy resolution at 78 MeV. π^- scattering at 80 MeV was also measured later[13] with resolution sufficient to discriminate against all nuclear excitations except the level at 0.48 MeV; this experiment reduced large-angle cross sections by a factor of about 3. Electron scattering data was used to argue that the contribution of the 0.48-MeV state is small. Thus at large angles the π^+ data give only upper bounds, and the π^- data may also contain some inelastic background. Calculating $\pi^\pm$ scattering with ρ_G and the theoretical parameters for Li^7, we obtained cross sections (see Fig. 7) which are too low for large angles for $\pi^\pm$, and too

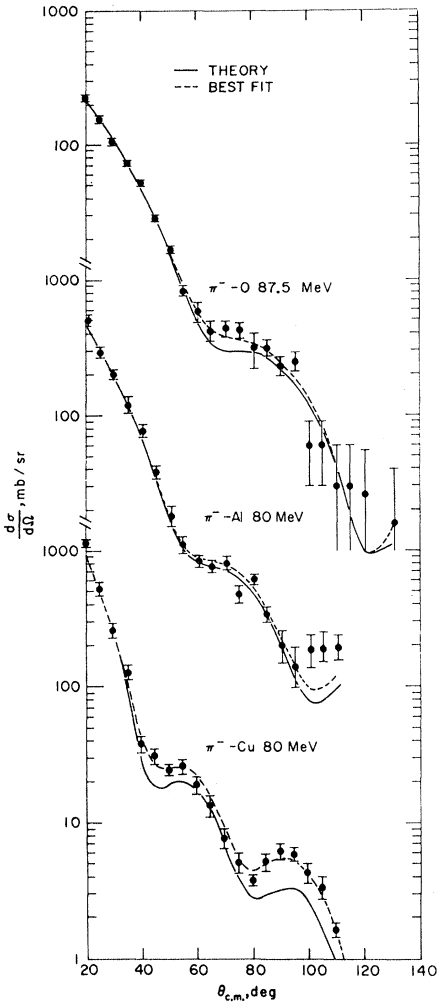

FIG. 6. π^- elastic scattering by copper and aluminum at 80 MeV, and by oxygen at 87.5 MeV. The 80-MeV experimental data are those of Baker *et al.* (Ref. 13), and contain some inelastic events; the oxygen data are those of Edelstein *et al.* (Ref. 14) and are pure elastic scattering. The theoretical parameters used were not adjusted for $A \neq 2Z$. They are $b_0 = -0.60 + 0.40i$, $b_1 = 6.30 + 1.80i$ for Cu and Al, and $b_0 = -0.60 + 0.38i$, $b_1 = 6.30 + 1.85i$ for O. Best-fit parameters are $b_0 = -0.64 + 0.15i$, $b_1 = 5.69 + 1.02i$ for Cu, $b_0 = -0.60 + 0.39i$, $b_1 = 6.26 + 1.44i$ for Al, and $b_0 = -1.12 + 0.28i$, $b_1 = 6.49 + 1.46i$ for O. Corresponding best-fit densities are Saxon-Woods densities with $R = 4.29$, $c = 0.50$ for Cu and $R = 3.12$, $c = 0.54$ for Al; for oxygen, the best density is a modified Gaussian with $a = 1.63$. The cross sections with theoretical parameters were evaluated with the same densities. The charge distributions used were uniform spheres with $R_c = 5.6$ for Cu and 4.2 for Al, and a modified Gaussian with $a_c = 1.6$ for O.

[25] P. P. Kane, Phys. Rev. **112**, 1337 (1958).
[26] J. Perry, thesis, University of Rochester, 1953 (unpublished); see also Ref. 25.
[27] R. E. Williams, W. F. Baker, and J. Rainwater, Phys. Rev. **104**, 1695 (1956).

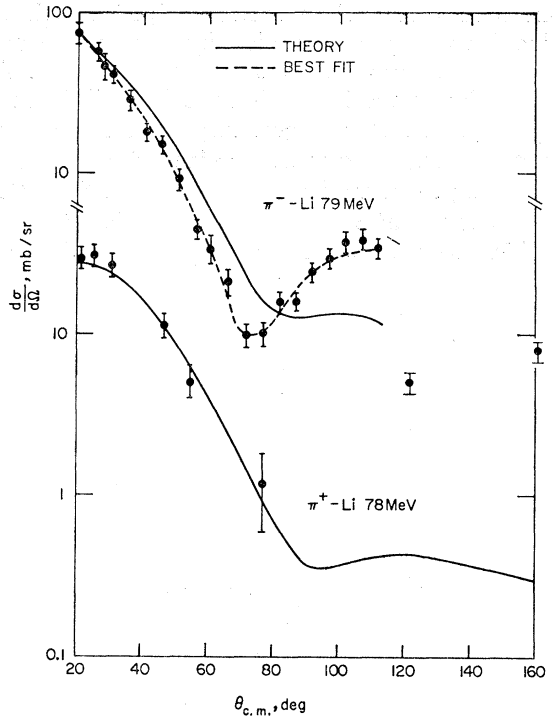

FIG. 7. π^+-lithium scattering at 78 MeV, and π^--lithium scattering at 79 MeV. All π^+ experimental data are those of Williams *et al.* (Ref. 27), and contain considerable inelastic background at large angles; π^+ data for angles less than 40° are also from Ref. 27. The remaining π^- data are 80-MeV measurements of Baker *et al.* (Ref. 27) which include elastic scattering plus excitation of the level at 0.48 MeV; they expect the latter cross section to be small, in analogy with electron scattering. Theoretical parameters are $b_0=-0.39+0.43i$, $b_1=6.22+1.79i$ for π^+, and $b_0=-0.84+0.43i$, $b_1=7.17+2.06i$ for π^-. Best-fit parameters for π^- are $b_0=-2.74-0.95i$, $b_1=7.56+1.02i$. A good fit to π^+-Li could not be found. A modified Gaussian nuclear density and charge distribution with $a=a_c=1.6$ was used in all calculations.

high for small angles for π^-. The search found a good fit for the π^-, but could not fit the poor π^+ data.

Helium: Published data on $\pi^\pm$ at 24 MeV [5] and π^+ at 48 and 66 MeV[28] have been studied, as well as preliminary unpublished $\pi^\pm$ data at 66 and 92 MeV.[29] The theoretical parameters and a Gaussian density yield curves which are too high for small angles and too low for large angles. Good fits were found in each case. However, the "best-fit" values of Re b_0 and Im b_1 did not approach the theoretical parameters as T_π increased, unlike other nuclei studied. See Figs. 8 and 9.

150-MeV Experiments: Fujii[17] has measured 150-MeV π^- scattering by C, Al, Cu, and Pb with an energy resolution of 10 MeV and an angular resolution of several degrees. For angles greater than 45°, he estimates that corrections for inelastic scattering are comparable to the measured cross sections. His attempts to fit the data with a simple density-proportional optical model led to cross sections too *large* for large angles; this is in contrast to the situation at lower energies[13] where the calculated results are too small for large angles. The Kisslinger model with theoretical parameters (which are quite different from those at lower energy) gives results which are somewhat *below* the data at large angles, but which are fairly good at small angles, as seen in Figs. 10 and 11. Because of the large inelastic component, we did not search extensively for phenomenological fits.

Budagov *et al.*[18] have studied elastic π^--helium interactions at 153 MeV in a cloud chamber. Our theoretical curve in Fig. 11 is below the data. A good fit was obtained with parameters much closer to those predicted at considerably *lower* energies.

Additional experimental data with good energy resolution in the energy region from 100 to 200 MeV are needed to determine the applicability of the model in this region.

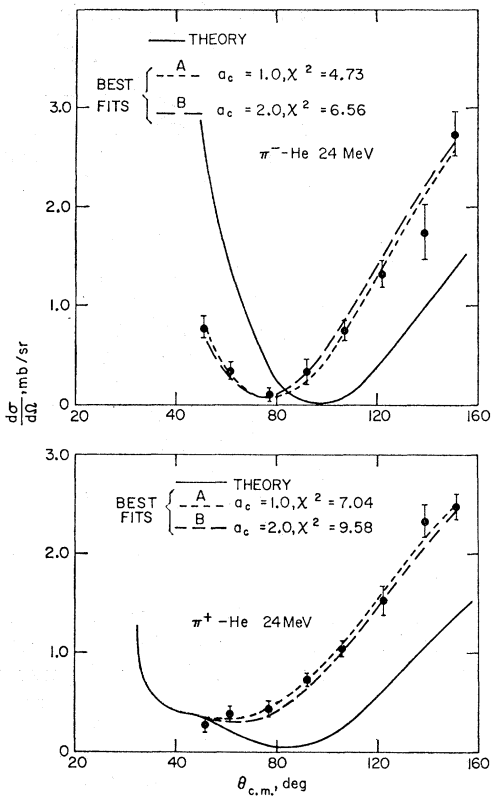

FIG. 8. π^+-helium elastic scattering at 24 MeV. Experimental data are from Nordberg and Kinsey (Ref. 5). Theoretical parameters used are $b_0=-0.03+0.55i$, $b_1=6.30+0.27i$; best-fit values are $b_0=-4.42+0.77i$, $b_1=6.06+0.13i$. A Gaussian nuclear density with $a=1.22$ is used for all calculations. The theoretical curves are based on a Gaussian charge distribution with $a_c=1.5$; the best-fit curves shown are for $a_c=1.0$ and 2.0. The best value for a_c is 1.03 ± 0.55, corresponding to $-2.4\leq r_\pi{}^2\leq 1.0$ (one standard deviation) or $r_\pi{}^2\leq 2.0$ (two standard deviations), in agreement with West's result (Ref. 8).

[28] M. M. Bloch, I. Kenyon, J. Keren, D. Koetke, P. K. Malhotra, R. Walker, and H. Wenzeler, in Proceedings of the Williamsburg Conference on Intermediate Energy Physics, Williamsburg, Virginia, 1966 p. 447 (unpublished).

[29] K. Crowe (private communication).

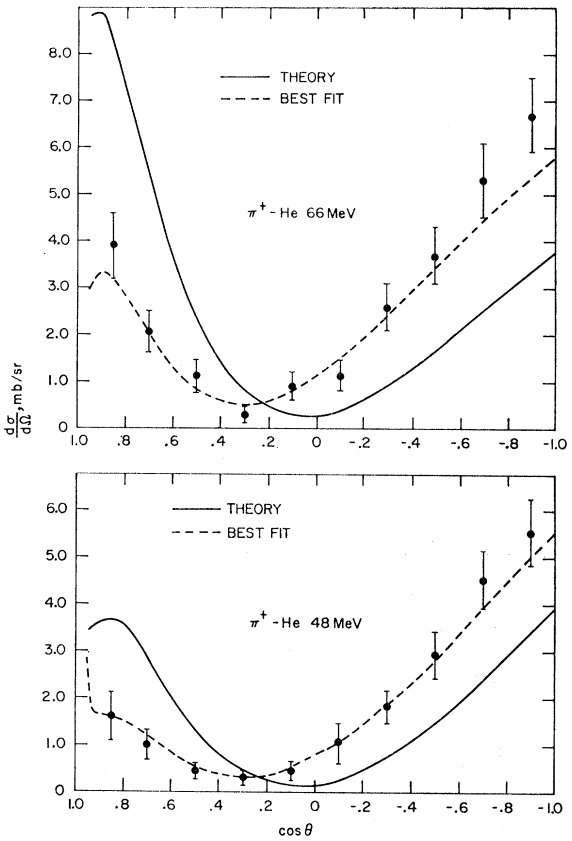

FIG. 9. π^+-helium elastic scattering at 48 and 66 MeV. Experimental data are those of Block *et al.* (Ref. 28). Theoretical parameters used are $b_0 = -0.80+0.48i$, $b_1 = 6.30+0.71i$ for 48 MeV, and $b_0 = -0.70+0.40i$, $b_1 = 6.30+1.20i$ for 66 MeV; best-fit parameters are $b_0 = -2.81+0.12i$, $b_1 = 5.94+0.24i$ for 48 MeV, and $b_0 = -2.57+0.09i$, $b_1 = 5.53+0.19i$ for 66 MeV. Gaussian densities with $a = 1.22$ and $a_c = 1.45$ were used.

Summary: We conclude that the Kisslinger model with theoretical parameters gives a qualitative fit to all the available data, and an excellent fit with phenomenological parameters in most cases. The theoretical curves give excellent fits for the energies and nuclei where one expected the approximations to be reasonably good.

IV. NUCLEAR DENSITIES AND RADII

An important result of our calculations is the systematic agreement of the nuclear parameters needed to fit pion scattering with those obtained from electron scattering. The best-fit density parameters were determined by varying them along with the potential parameters b_0 and b_1 when the data had good statistics and energy resolution.

The 80-MeV π^--C data were fitted both with ρ_G and with ρ_s in an attempt to observe a shape dependence, i.e., to determine a second density parameter. Excellent agreement was found with ρ_G for $a = 1.47$ (rms radius $\bar{r} = 2.14$) using b's close to the theoretical values. Using ρ_s, a search begun at $c = 0.5$ led to an equally good fit with $c = 0.45$, $R = 1.97$ ($\bar{r} = 2.26$). Comparison of the two cross-section curves showed them to be nearly identical; the two densities were also quite similar when plotted.

Unfortunately, this remarkable result was fortuitous, since fixing c at 0.25 led again to an equally good fit for $R = 2.45 \pm 0.11$ ($\bar{r} = 2.11 \pm 0.10$). The last density is

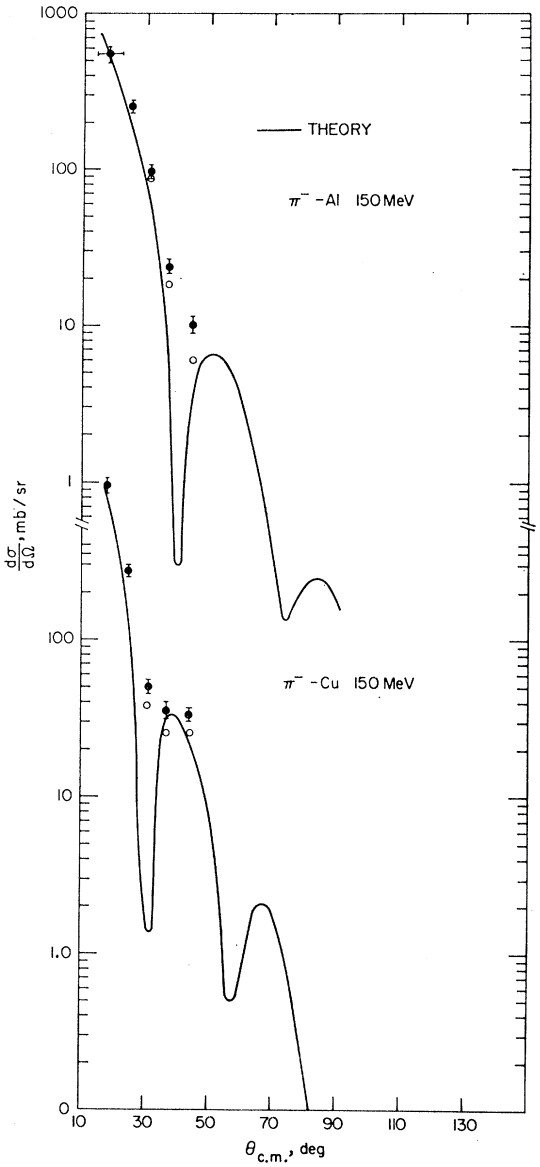

FIG. 10. π^- elastic scattering by copper and aluminum at 150 MeV. Experimental data are those of Fujii (Ref. 17); he estimates with a model that subtraction of inelastic contributions would give the cross sections indicated by open circles. The theoretical parameters used are $b_0 = -0.60+0.30i$, $b_1 = 4.70+7.0i$. We have not folded the experimental angular resolution into the calculated curves nor searched extensively for phenomenological fits. Saxon-Woods nuclear densities with $R = 4.3$, $c = 0.5$ and $R = 3.3$, $c = 0.5$ and uniform sphere charge distributions with $R_c = 6.0$ and $R_c = 4.2$ were used for Cu and Al, respectively.

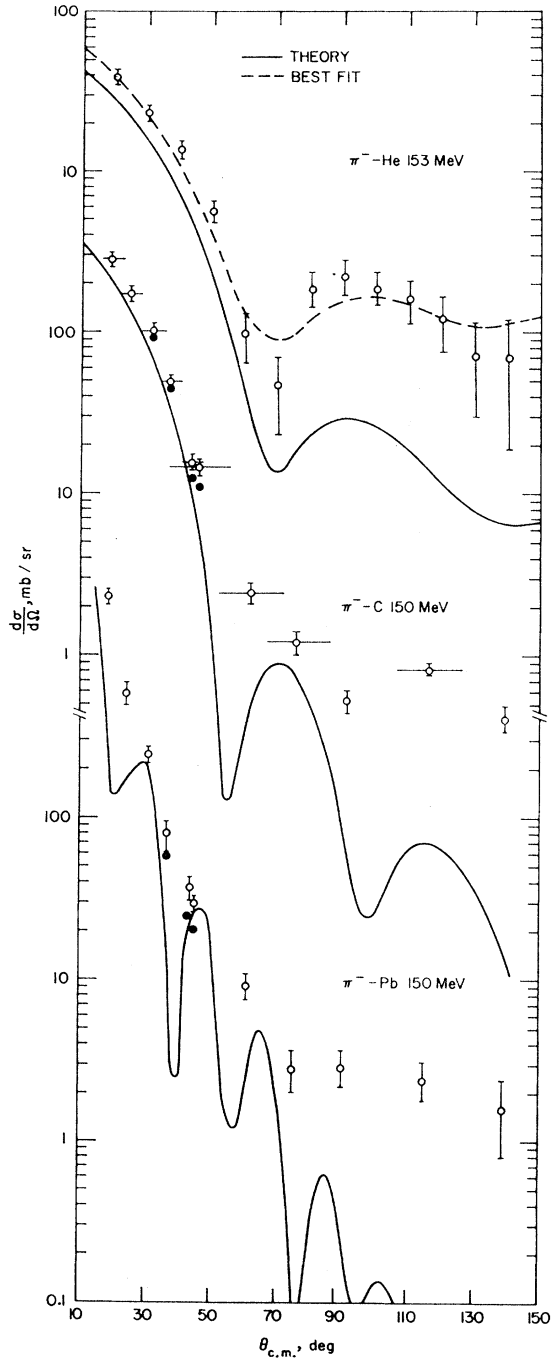

FIG. 11. π^- elastic scattering by lead and carbon at 150 MeV, and by helium at 153 MeV. The experimental data for Pb and Cu are those of Fujii (Ref. 17), and the He data are the elastic cross sections of Budgov *et al.* (Ref. 18). Approximate corrections fo Pb and Cu inelastic events give the cross sections indicated by black circles; for large angles, the estimated corrections are comparable to the data. Theoretical parameters are $b_0=-0.60+0.30i$, $b_1=4.70+7.0i$; best-fit values for He are $b_0=-1.09-1.02i$, $b_1=5.27+0.18i$. We used a Saxon-Woods nuclear density with $R=6.4$, $c=0.5$ and a uniform-sphere charge density with $R_c=8.4$ for lead, a modified Gaussian with $a=1.55$, $a_c=1.65$ for carbon, and a Gaussian with $a=1.22$, $a_c=1.50$ for helium.

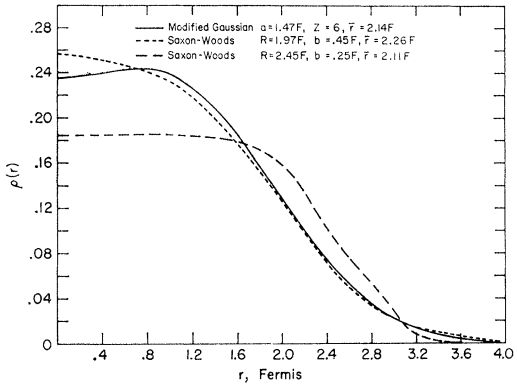

FIG. 12. Three densities for carbon giving equally good fits to the 80-MeV data (see Fig. 4): Modified Gaussian, $a=1.47$, $\bar{r}=2.14$; Saxon-Woods, $R=1.97$, $c=0.45$, $\bar{r}=2.26$; Saxon-Woods, $R=2.45$, $c=0.25$, $\bar{r}=2.11$.

somewhat different from the first two, as is seen in Fig. 12. (It is interesting that Baker *et al.*[13] obtained $c=0.25$, $R=1.08A^{1/3}=2.48$ with the modified Kisslinger model, in excellent agreement with our last result.)

The three densities give consistent results for $\bar{r}$, and agree very well with the values $a=1.47$ and 1.49 found at 69.5 and 87,5 MeV respectively, and also with the electron-scattering[23] value $a=1.55$ (1.60 before correcting for finite proton size). Furthermore, the Saxon with $c=0.25$ did give a much larger cross section than the other densities for angles near the second minimum. (See Fig. 4.) Thus experiments with good energy resolution at large angles could distinguish between these densities and determine a second density parameter.

Best Gaussian fits to the helium data gave values for a between 1.22 and 1.27; the electron-scattering[30] value is 1.22 (1.35 less proton size correction). The 80-MeV Al and Cu Saxon-Woods fits correspond to $R=1.10A^{1/3}$ and $1.08A^{1/3}$, respectively; the average electron-scattering[23] result is $(1.07\pm0.02)A^{1/3}$. The best c's are also comparable to those found in electron scattering. Our modified Gaussian fit for oxygen gives $a=1.63$; the electron-scattering[23] result is 1.67 (1.72 less proton size correction).

Thus all the pion-scattering radii are in excellent agreement with electron-scattering data. The results obtained so far indicate that additional experimental and theoretical work may lead to useful new information about nuclear densities.

V. PION CHARGE RADIUS

The contribution of the pion charge radius to $\pi^{\pm}$-α scattering was calculated by assuming a Gaussian charge density for each particle. This is equivalent to a point charge and a single Gaussian $\exp[-r^2/a_c^2]$, where

[30] R. Herman and R. Hofstadter, *High Energy Electron Scattering Tables* (Stanford University Press, Stanford, California, 1960).

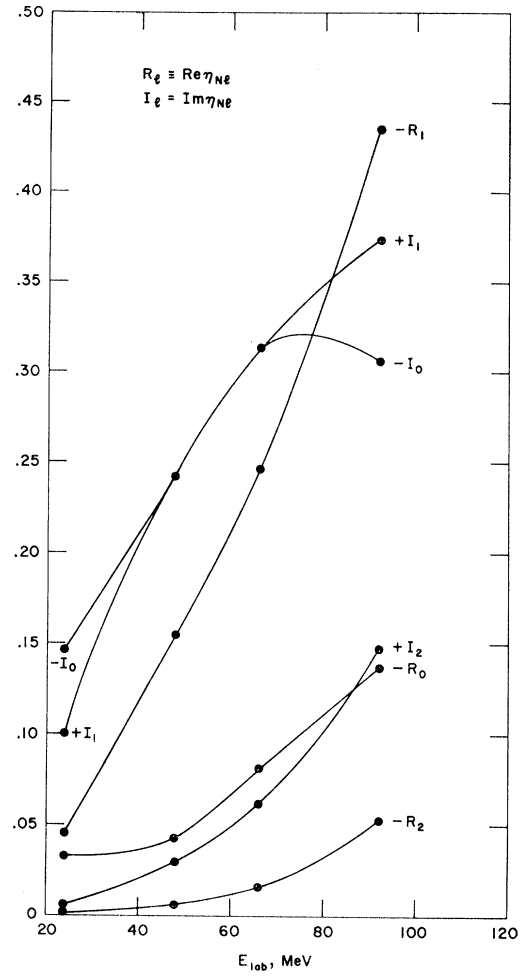

FIG. 13. Amplitudes obtained from optical-model analysis of π-helium scattering at 24, 48, 66, and 92 MeV (Refs. 5, 28, 29). See Sec. V of text.

$a_c^2 = a_\alpha^2 + a_\pi^2$, and the rms pion radius is

$$r_\pi = [1.5(a_c^2 - a_\alpha^2)]^{1/2}. \quad (29)$$

Electron scattering gives[30] $a_\alpha = 1.35$, so that a measurement of a_c determines r_π.

In the Introduction we noted that a Born-approximation Coulomb amplitude plus a phase-shift expansion for f_N will lead to erroneous results for r_π if the distortion amplitude f_D is comparable to the contribution of the pion charge distribution. We calculated f_D as follows The optical parameters were varied so as to obtain a fit to the $\pi-\alpha$ data at 24, 48, 66, and 92 MeV.[5,28,29] The partial-wave amplitudes $f_l^\pm$ thus obtained for $\pi^\pm$ were compared to those found with no nuclear forces, i.e., with only Coulomb forces; the latter satisfied $|f_{Cl}^+| - |f_{Cl}^-| \approx 0$, as expected. The nuclear and distortion amplitudes were then found from

$$f_{Dl} = \tfrac{1}{2}(f_l^{(+)} - f_l^{(-)} - 2f_{Cl}), \quad (30)$$

$$f_{Nl} = \tfrac{1}{2}(f_l^{(+)} + f_l^{(-)}). \quad (31)$$

It is convenient to write the amplitude as

$$f^{(\pm)}(\theta) \equiv \sum f_l^{(\pm)} P_l(\cos\theta)(2l+1) = (1/2ip) \times \sum (\eta_{Nl} \pm \eta_{Dl} \pm \eta_{Cl}) P_l(\cos\theta)(2l+1) \pm f_{C0}(\theta),$$

where η_{Nl}, η_{Dl}, and η_{Cl} correspond to f_N, f_D, and $\Delta f_C \equiv f_C - f_{C0}$, respectively. We found that η_{Nl} and η_{Dl} are nearly independent of a_c (or r_π). At each energy, several slightly different optical-parameter sets gave the same χ^2; all of these gave the same η_{Dl}. The variations in η_{Dl} due to changes in r_π or in the choice of optical parameters are ≤ 0.001, and are negligible.

Figure 13 gives the η_{Nl}'s, and Fig. 14 gives Im η_{C0} for three r_π values as well as the η_{Dl}'s. The distortions are small compared to the η_{Nl}'s, but are larger than the variation in Im η_{C0} due to changes in r_π.

If we take into account only Im η_{D0}, which interferes directly with the form-factor term Im η_{C0}, the 24-MeV result for r_π is considerably altered. Instead of

$$r_\pi = 1.8 \pm 0.8 \quad \text{or} \quad 1.0 \leq r_\pi^2 \leq 6.76, \quad (3)$$

we find

$$-0.8 \leq r_\pi^2 \leq 4.0.$$

Furthermore, if we include all the distortion effects by fitting our optical-model calculations directly to the

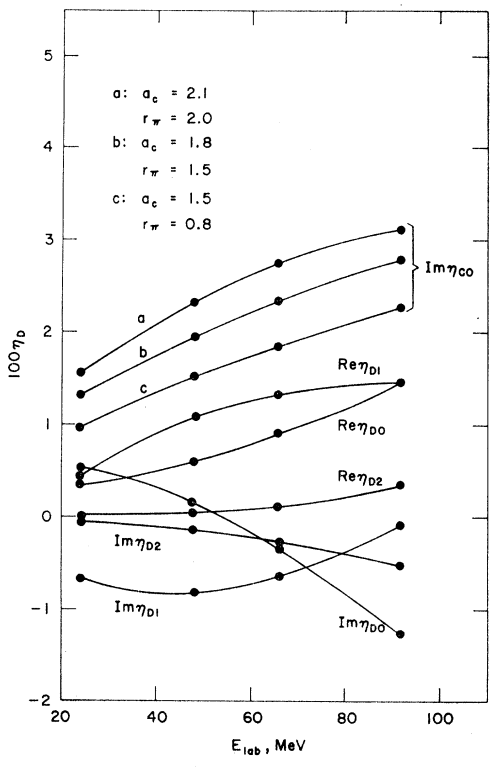

FIG. 14. Distortion amplitudes η_{Dl} and finite-size Coulomb amplitudes η_{Cl} obtained from optical-model analysis of π-helium scattering. See Fig. 13 and Sec. V of text.

$\pi^{\pm}$ data, we find (see Fig. 8) the best fit at $a_c=1.03 \pm 0.55$, or

$$-2.4 \leq r_\pi^2 \leq 1.0 \quad \text{(1 std. dev.)}$$

or, corresponding to $a_c=2.13$,

$$r_\pi \leq 2.0 \quad \text{(2 std. dev.)} \quad (32)$$

in complete agreement with West's conclusions.[8] Note that at this energy the cross sections are sensitive to r_π at all angles.

In a future paper, we will present a determination of r_π from Crowe's data[29] and a discussion of the optimum energies for further study of the pion form factor.

ACKNOWLEDGMENTS

It is a pleasure to acknowledge valuable conversations with Professor R. Hofstadter, Professor M. Block, and Professor K. Crowe. Part of this work was done while two of us (DMF and MMS) were summer visitors at Brookhaven National Laboratory. The computations were done at the MIT Laboratory for Nuclear Science, Brookhaven National Laboratory, and the University of Massachusetts at Amherst. We would like to acknowledge a grant of funds for computer time from the University of Massachusetts, and to thank the staffs of all three computer centers for their valuable assistance.

PHYSICAL REVIEW VOLUME 162, NUMBER 5 25 OCTOBER 1967

General Sum Rules and the Form of the Equal-Time Commutator*

M. O. TAHA

Department of Applied Mathematics and Theoretical Physics, University of Cambridge, Cambridge, England

(Received 11 May 1967)

Using a method introduced in a previous paper, we define covariant functions corresponding to the retarded product and the equal-time commutator. From these we obtain general sum-rule identities, employing three independent infinite limits. These identities considerably limit the form of the equal-time commutator. The simplest form consistent with the general covariance properties is discussed.

I. INTRODUCTION

A METHOD has been introduced in a recent paper[1] for the manipulation of the retarded product, the equal-time commutator, and the related functions in the theory of currents. It provides an understanding of the manner in which the argument of the integrand (in integrals from which these functions are obtained) varies during the integration. This clearly indicates three independent infinite limits in which the functions can be evaluated, with all the external invariants kept finite, and with the integration contour running along the real axis of one invariant (the integration variable) while the remaining invariants are kept fixed.

To keep the discussion simple, conditions have been imposed in Ref. 1 to ensure the covariance of the retarded product of two vector currents. Under these restrictions, and with the assumptions of convergence of the integrals and vanishing contributions from infinite-mass intermediate states, conditions for the equivalence of the three limits have been obtained. Such conditions are based on the fact that an expression for an invariant or a covariant function obtained in any one limit, for all finite physical values of the invariants, and taking a form explicitly independent of the limit, must continue to hold in general and be equivalent to a similar expression obtained in another limit. These conditions of equivalence are very fruitful since they immediately generalize results obtained in one limit, and simultaneously considerably limit the form of the functions involved.[1,2] This last consequence allows sum rules for the strong interactions completely independent of current algebra.

It is our purpose in the present paper to remove the conditions that have been imposed in Ref. 1 to ensure a covariant retarded product and treat the general case by the same method. When the retarded product is no longer covariant, and still figures in the formalism, one has to satisfactorily define in terms of it a covariant function that represents the amplitudes for the scattering processes. (We refer here to the weak and electromagnetic interaction amplitudes). In Sec. II we define such functions employing the three infinite limits and the method of Ref. 1. This amounts to the construction of invariant and covariant functions corresponding to the retarded products. We then construct a covariant function C_ν^{ij} corresponding to the Fourier transform $E_{0\nu}^{ij}$ of the equal-time commutator involving the time component.

The equivalence conditions are then derived in Sec.

* Research sponsored in part by the Air Force Office of Scientific Research under Grant No. AF EOAR 65-36 through the European Office of Aerospace Research (OAR), U. S. Air Force.

[1] M. O. Taha, Cambridge University Report, 1967 (unpublished).

[2] M. O. Taha, Cambridge University Report, 1967 (unpublished).